Journal of Electrical Engineering, Electronics, Control and Computer Science – JEEECCS, Volume 7, Issue 25, pages 19-28, 2021

Synergetic control theory scheme for asynchronous generator based dual-rotor wind power

Habib Benbouhenni
Labo. LAAS, Departement de Génie Électrique
ENPO-MA, Oran, Algeria
habib0264@gmail.com

***Abstract* – This paper presents a new direct active and reactive powers command (DARPC) method for an asynchronous generator (ASG) based dual-rotor wind energy (DRWE) system. Switching vectors for rotor side converter were selected from the modified neural space vector pulse width modulation (MNSVPWM) using the estimated rotor flux position and the errors of the active and reactive power. Using a proportional-integral controller may cause undesired stator current and power oscillation. In this work, the reduced oscillations of active and reactive powers with the application of the synergetic control theory (SYC) will be presented. Then a new DARPC strategy will be proposed. The principle of the schematic and the disadvantages or advantages of the designed technique are proposed. Simulation results of a 1.5 MW ASG system demonstrate the performances, robustness, and effectiveness of the designed technique during variations of ASG parameters, and reactive and active powers.**

Keywords-DARPC, DRWE, ASG, SYC, MNSVPWM

I. INTRODUCTION

Compared to the classical nonlinear strategies, synergetic control (SYC) theory has many advantages leading to high efficiency, such as fast response dynamic, very easy algorithm, and does not need the mathematical model of the system [1]. This theory has been applied in many scientific works [2-12].

The direct active and reactive powers command (DARPC) technique is used in numerous of the works [13-24]; however, one of its disadvantages is that the oscillations in active and reactive powers, which may affect the functioning of the converter, the generator and even the effectiveness of the system as a whole. It is shown that the DARPC method with constant switching frequency is mainly achieved by using the SVM, PWM, P-DARPC, and DSVM-DARPC respectively. On the other hand, large waves of active power ripple reduce the life cycle and stress of the system (regular maintenance). Despite the above problems, the DARPC strategy remains one of the best-recommended solutions for asynchronous generator control. compared with the field-oriented control (FOC), the DARPC is a robust strategy, easy to apply, uncomplicated algorithm, and minimizes the oscillations of active and reactive powers of the ASG relative to FOC strategy [25].

Our work objective is to propose a robust SYC technique to improve the performance of the DARPC method with no overshoot and to ensure a good tracking of the desired trajectory in the presence of external disturbances. Using our neural modified SVPWM technique (NMSVPWM) to determine the optimal controller parameters (gains) enables its desired performance.

II. DRWP MODEL

The DRWT system uses two wind turbines rotating in opposite directions on the same axis. The DRWT system has been proposed as new wind energy, as shown in Figure 1. The DRWT system is a wind turbine used to generates electrical power. DRWP system has a high energy conversion comparing with other types and renewable resources. The DRWT system gives more aerodynamic torque and power coefficient compared to the single-rotor wind turbine system. The DRWT system design is composed of two wind turbines, the main one and the auxiliary turbines [26]. The control of the DRWT system is difficult compared to the single-rotor wind turbine system. The total aerodynamic power of the DRWT system is given by the main turbine power (P_M) together with the auxiliary turbine power (P_A) as shown by the following equation:

$$P_{DRWT} = P_T = P_M + P_A \quad (1)$$

Where: P_M: Main turbine power.
P_A: auxiliary turbine power.
P_T: total aerodynamic power.

The total torque of the DRWT system is given:

$$T_T = T_M + T_A \quad (2)$$

Where: T_M: Main turbine torque.
T_A: Auxiliary turbine torque.
T_T: Total aerodynamic torque.

The aerodynamic torque of the auxiliary and main turbines are given [27]:

$$T_A = \frac{1}{2\lambda_A^3}.\rho.\pi.R_A^5.C_p.w_A^2 \quad (3)$$

$$T_M = \frac{1}{2\lambda_M^3}.\rho.\pi.R_A^5.C_p.w_M^2 \quad (4)$$

With R_A, R_M: Blade radius of the main and auxiliary turbines, λ_A, λ_M: the tip speed ration of the main and auxiliary turbines, ρ: the air density and w_M, w_A the mechanical speed of the main and auxiliary turbines.

The tip speed ratios of the auxiliary and main turbines are given:

$$\lambda_A = \frac{w_A.R_A}{V_1} \quad (5)$$

$$\lambda_M = \frac{w_M.R_M}{V_M} \quad (6)$$

Where V_1 is the wind speed on an auxiliary turbine and V_M is the speed of the unified wind on main turbine.

The wind speed at any point between the auxiliary and main blades is given:

$$V_x = V_1(1-\frac{1-\sqrt{(1-C_T)}}{2}(1+\frac{2.x}{\sqrt{1+4.x^2}})) \quad (7)$$

With x: the non-dimensional distance from the auxiliary rotor disk, Vx the velocity of the disturbed wind between rotors at point x and C_T the trust coefficient, which is chosen to be 0.9. [28].

Equation (8) shows the power coefficient function, β is pitch angle

$$C_p(\lambda,\beta) = 0.517(\frac{116}{\lambda_i} - 0.4\beta - 5)e^{-\frac{21}{\lambda_i}} + 0.0068\lambda \quad (8)$$

With:

$$\frac{1}{\lambda_i} = \frac{1}{\lambda + 0.08\beta} - \frac{0.035}{\beta^3+1} \quad (9)$$

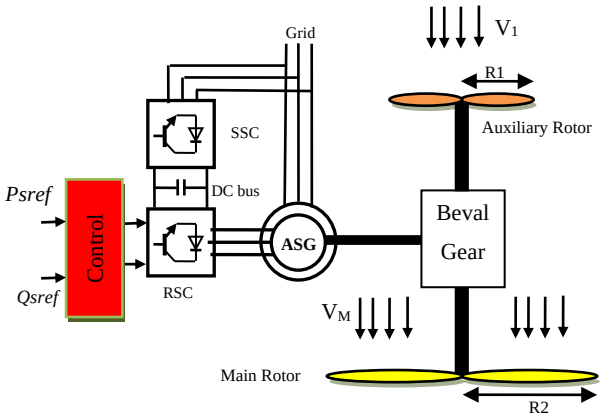

Figure 1. Block diagram of DRWT with a ASG.

III. ASG MODEL

This section provides the mathematical model of the ASG using Park transformations. The equivalent two-phase model of the ASG, represented in an arbitrary rotating (q-d) reference frame is [29, 30]:

$$\begin{cases} V_{dr} = R_r I_{dr} + \frac{d}{dt}\psi_{dr} - (w_r - w_s)\psi_{qr} \\ V_{qr} = R_r I_{qr} + \frac{d}{dt}\psi_{qr} + (w_r - w_s)\psi_{dr} \end{cases} \quad (10)$$

$$\begin{cases} V_{ds} = R_s I_{ds} + \frac{d}{dt}\psi_{ds} - \omega_s\psi_{qs} \\ V_{qs} = R_s I_{qs} + \frac{d}{dt}\psi_{qs} + \omega_s\psi_{ds} \end{cases} \quad (11)$$

The quadrature and directe components flux can be obtained by:

$$\begin{cases} \psi_{dr} = L_r I_{dr} + MI_{dr} \\ \psi_{qr} = L_r I_{qr} + MI_{qr} \end{cases} \quad (12)$$

$$\begin{cases} \psi_{ds} = L_s I_{ds} + MI_{dr} \\ \psi_{qs} = L_s I_{qs} + MI_{qr} \end{cases} \quad (13)$$

The torque of ASG are defined as:

$$T_e = \frac{3}{2}p\frac{M}{L_r}(I_{dr}.\psi_{qs} - I_{qr}.\psi_{ds}) \quad (14)$$

The active and reactive powers are given as:

$$\begin{cases} P_s = \frac{3}{2}(V_{ds}I_{ds} + V_{qs}I_{qs}) \\ Q_s = \frac{3}{2}(V_{qs}I_{ds} - V_{ds}I_{qs}) \end{cases} \quad (15)$$

The mechanical model of the DFIG can be written as follows:

$$T_e - T_r = J\cdot\frac{d\Omega}{dt} + f\cdot\Omega \quad (16)$$

Where: Ω is the mechanical rotor speed, J is the inertia, f is the viscous friction coefficient, T_r is the load torque.

IV. NEURAL MODIFIED SVPWM TECHNIQUE

The SVPWM technique based on calculating the angle and sector has some advantages such as minimizing the harmonic distortion of current and giving 15% more voltage output compared to the classical PWM strategy. But this strategy is difficult to implement compared to the PWM strategy. In [31], the authors proposed a new SVPWM principle based on calculating the minimum and maximum of three-phase voltages (Va, Vb, Vc), as presented in Figure 2. This proposed strategy is easy and has a simple structure [32].

In order to obtain a robust modulation strategy of RSC inverter, in any control, it is must to use the neural networks to produce a robust strategy. The basic idea of the neural SVPWM technique is to replace the classical hysteresis comparators with neural algorithms [33]. The neural SVPWM technique is designed to control the RSC of the ASG-

based DRWP system and generate the rotor voltage reference components, as shown in Figure 3. A proposed SVPWM technique is proposed to minimize torque, flux, current and power ripples. This proposed SVPWM technique is obtained by replacing the hysteresis comparators with the neural controllers.

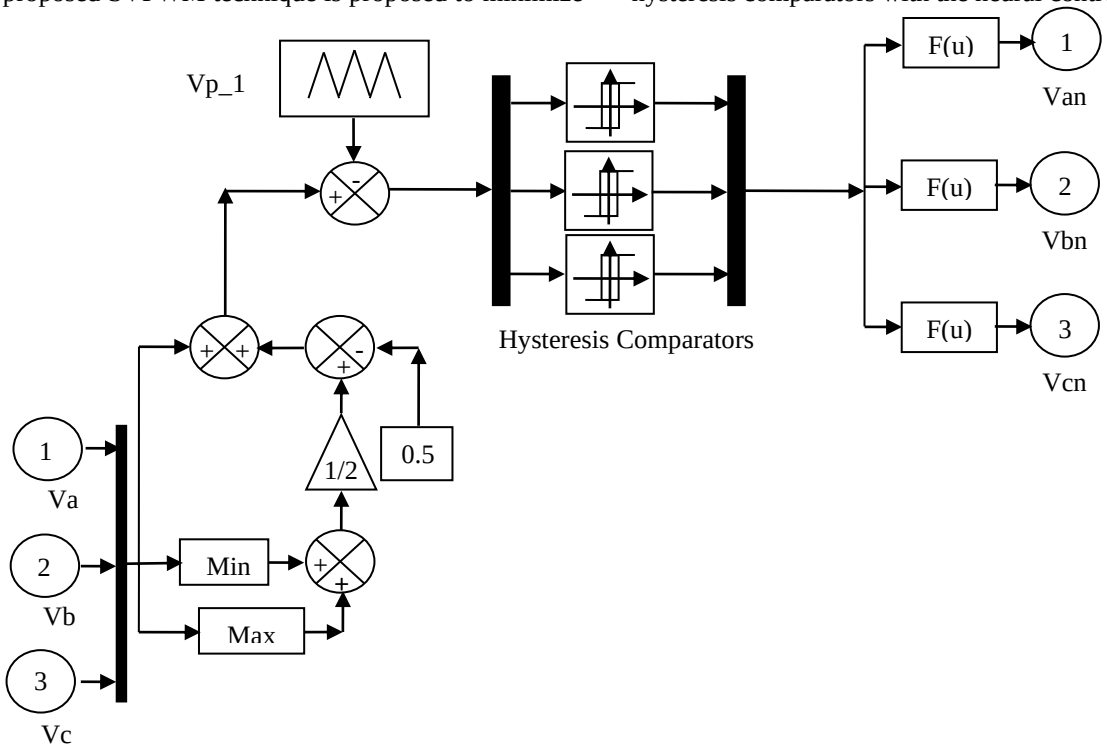

Figure 2. Modified SVPWM technique.

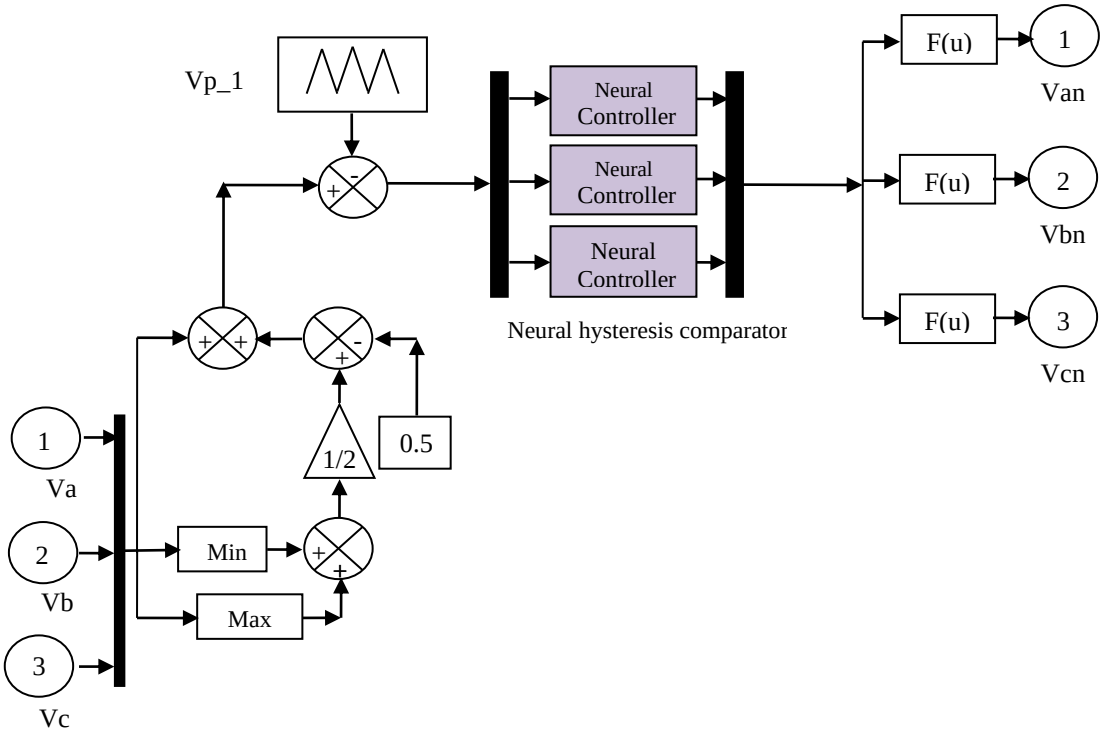

Figure 3. Neural modified SVPWM technique.

In order to design the neural controllers, we used the Levenberg-Marquardt backpropagation. This algorithm is an easy, robust and simple algorithm. The schematic diagram of the neural controller with the Levenberg-Marquardt algorithm is shown in Figure 4. The neural controllers consist of a hidden layer, output layer, and input layer. However, the hidden layer has 8 neurons. Table 1 shows the parameters of the neural controller. The schematic diagram of layer 1 and layer 2 and is shown in Figure 5 and Figure 6 respectively.

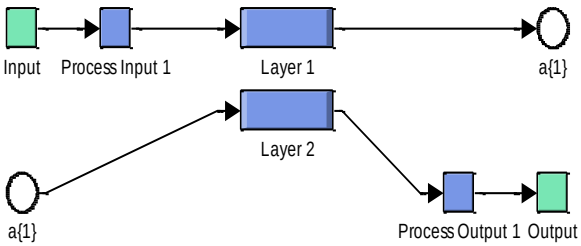

Figure 4. Internal structure of the neural hysteresis controllers.

TABLE I. PARAMETERS OF THE NEURAL CONTROLLER

Parameters	Values
Functions of activation	Tensing, Purling, Gensim
TrainParam.Lr	0.02
Number of neurons of hidden layer	8
TrainParam.show	50
TrainParam.mu	0.9
Number of neurons of input layer	1
Number of neurons of output layer	1
Algorithm	Levenberg-Marquardt
Coeff of acceleration of convergence (mc)	0.9
TrainParam.goal	0
TrainParam.eposh	300
Number of hidden layers	1

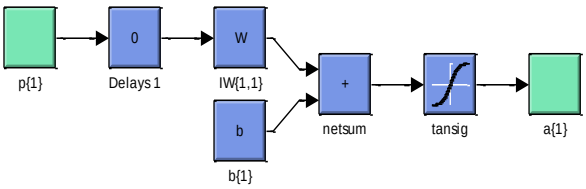

Figure 5. Structure of Layer 1.

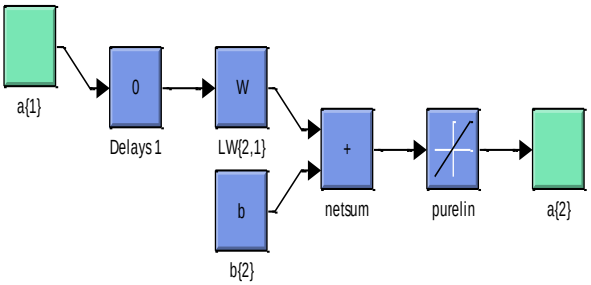

Figure 6. Structure of Layer 2.

V. DPC CONTROL WITH PI CONTROLLERS

The following figure (Figure 7) shows the operating principle of DARPC control of the asynchronous generators. The direct axis voltage is used to control the reactive power and the quadratic axis voltage is used to control the active power. For fixed switching frequencies, the neural modified SVPWM technique is used to control the RSC inverter. Several literature studies to explore the performance of the DARPC technique based on lookup tables have been published recently [34-36]. The important advantage of using the DARPC method is given by the fact that it is a simple method, has a robust control. but the DARPC strategy has a well-known disadvantage such as reactive power oscillation, current oscillation, and active power oscillation [37]. In classical DARPC control, two hysteresis comparators have been used to control the active and reactive power and one lookup table is used to control the RSC inverter. There is another method of DARPC control using two proportional-integral (PI) controllers and the classical SVPWM technique. This proposed method has more advantages and solves the problems found in the classical method. The DARPC with PI controllers and SVPWM technique reduces the active power oscillation, current oscillation, torque oscillation, and reactive power oscillation compared to DARPC with a lookup table. As well as DARPC control using PI controllers that are not affected much by change parameters of the machine, unlike the classical method, which is affected by change parameters this is evident in the great value of the oscillation in both active and reactive powers.

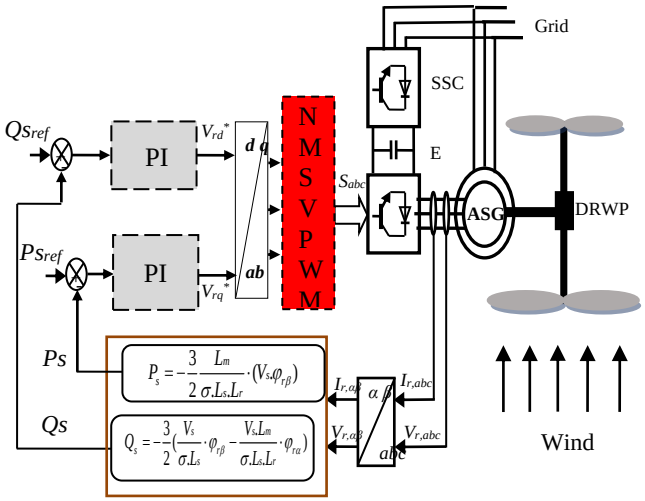

Figure 7. DARPC strategy PI controllers.

The developed system in Figure 7 is used for reducing the active and reactive powers oscillation. The estimated reactive and active powers are given as:

$$Q_s = -\frac{3}{2}\left(\frac{V_s}{\sigma.L_s}\cdot\varphi_{r\beta} - \frac{V_s.L_m}{\sigma.L_s.L_r}\cdot\varphi_{r\alpha}\right) \quad (14)$$

$$P_s = -\frac{3}{2}\frac{L_m}{\sigma.L_s.L_r}\cdot(V_s.\varphi_{r\beta}) \quad (15)$$

Where:

$$\Psi_{s\beta} = \sigma L_r I_{r\beta} \quad (16)$$

$$\Psi_{s\alpha} = \sigma L_r I_{r\alpha} + \frac{M}{L_s}\Psi_s \quad (17)$$

$$\sigma = 1 - \frac{M^2}{L_r L_S} \tag{18}$$

VI. SYNERGETIC-DIRECT ACTIVE AND REACTIVE POWERS CONTROL

The proposed synergetic based DARPC technique includes a synergetic controller block used to produce direct and quadrature rotor voltages (Vqr and Vdr). The direct and quadrature rotor voltages are calculated by synergetic control using instantaneously active and reactive power errors. The schematic block of the proposed system is given in Figure 8. A neural SVPWM technique is used to provide the switching patterns of the RSC inverter with a constant switching frequency. The active power is estimated using (15) and reactive power is estimated using (14). It is shown that the designed technique is less complicated compared with other techniques such as FOC technique or vector control, where the PI controllers are eliminated. On the other hand, the proposed strategy reduced the active and reactive oscillations compared with DARPC strategy with PI controllers.

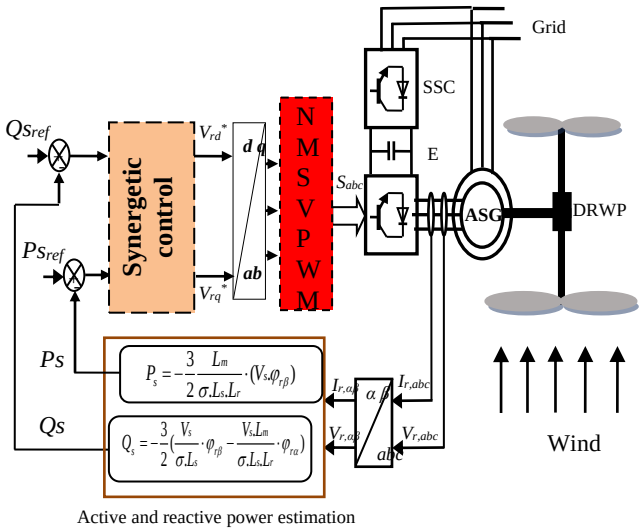

Figure 8. DARPC with synergetic control.

There are several non-linear methods used in the field of electrical engineering, especially in the field of electrical machinery control, among the most famous of which we find sliding control, and this is due to its advantages that it is distinguished by, like other methods, this method is characterized by solidity and ease of achievement and can be applied to all electrical machines. But in recent years, a new theory has appeared under the name of Synergetic Control, which has almost the same advantages as sliding control in terms of rigidity, ease of implementation, and not being affected by the change of machine parameters such as resistances. Synergetic control was developed by Kolesnikov and his Coworkers. This new method is based on modern mathematics. This technique is applicable to the dynamic control of nonlinear, and high-dimensional systems. The major idea of synergetic control is to confine the motion or trajectories of the system to a hyperplane. This technique is similar to sliding control in the way the hyperplane is being constructed. The synergetic control is defined as follows [38]:

$$T.\frac{d\Psi}{dt} + \Psi = 0 \tag{19}$$

Where, the ψ is the macro variable, T is the rate of convergence of the system.

The solution of Eq. (16) is given by:

$$\Psi(t) = \Psi_0 \dot{e}^{t/T} \tag{20}$$

In synergetic DARPC strategy, two synergetic controllers are used to control the active and reactive of ASG-based DRWP systems. The active power regulator generates the reference voltage Vqr*. The macro-variable for active power controller is defined by:

$$\Psi = P_{sref} - P_s \tag{21}$$

Then the derivative of it is given by:

$$\dot{\Psi} = \dot{P}_{sref} - \dot{P}_s \tag{22}$$

The synergetic active power controller can be seen in Figure 9.

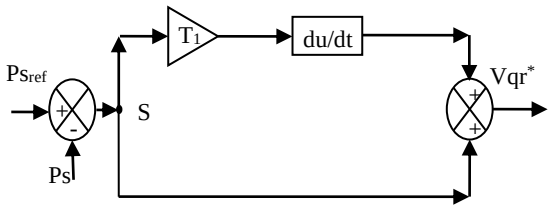

Figure 9. Structure of the command law of the synergetic active power controller.

The synergetic-reactive power regulator generates the reference voltage Vdr*. The macro-variable for reactive power controller is defined by:

$$\Psi = Q_{sref} - Q_s \tag{23}$$

Then the derivative of it is given by:

$$\dot{\Psi} = \dot{Q}_{sref} - \dot{Q}_s \tag{24}$$

The synergetic-reactive power controller can be seen in Figure 10.

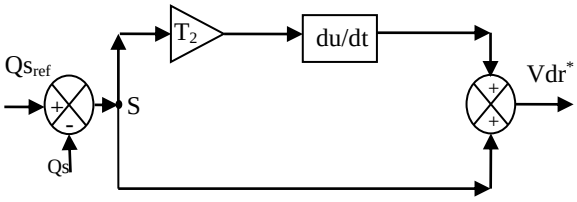

Figure 10. Structure of the command law of the synergetic reactive power controller.

VII. RESULTS AND ANALYSIS

The simulation results of the synergetic-direct active and reactive powers control strategy using the neural modified SVPWM strategy (DARPC-SYC) of the ASG-based DRWP system are compared with the traditional DARPC with PI controllers.

A. First Test

The simulation waveforms of the reference and measured active power of the ASG-based DRWP system are shown in Figure 11 in order to compare the performance of the DARPC-SYC technique with the performance of the DARPC with PI controllers. The active power tracks almost perfectly their reference value ($P_{s\text{-}ref}$). On the other hand, the amplitudes of the oscillations of the active power are smaller and occur in a shorter time period in comparison with the oscillations obtained for the DARPC-SYC technique (Figure 15).

For the DARPC-SYC and DARPC technique with PI controllers, the reactive power track almost perfectly their reference value (Figure 12). Moreover, the DARPC-SYC technique minimized the reactive power oscillation compared to the DARPC with PI controllers (Figure 16).

The waveforms of the torque of both control schemes are shown in Figure 13. The amplitudes of the torque depending on the state of the drive system and the value of the load active power. The proposed command scheme minimized the torque compared to the DARPC with PI controllers (see Figure 17).

Figure 19 and Figure 20 show the THD value of the DARPC with PI controllers and DARPC-SYC technique respectively. It can be clearly observed that the THD value is minimized for the DARPC-SYC technique (THD = 0.40%) when compared to the DARPC with PI controllers (THD =0.58%).

The trajectory of the measured magnitude of the stator current is shown in Figure 14. It can be stated that the amplitudes of the stator currents depend on the state of the drive system and the value of the load active/reactive power of the ASG-based DRWP systems. In addition, the DARPC with PI controllers gives more ripple in current compared to the DARPC-SYC technique (Figure 18). On the other hand, the DARPC-SYC technique minimized more the response time of the torque, active and reactive powers compared to the DARPC with PI controllers (Table 2).

TABLE II. COMPARATIVE ANALYSIS OF RESPONSE TIME

	Response time		
	Torque	**Active power**	**Reactive power**
DARPC-PI	0.036s	0.036s	0.014s
DARPC-SYC	1.78ms	1.78ms	8.5ms

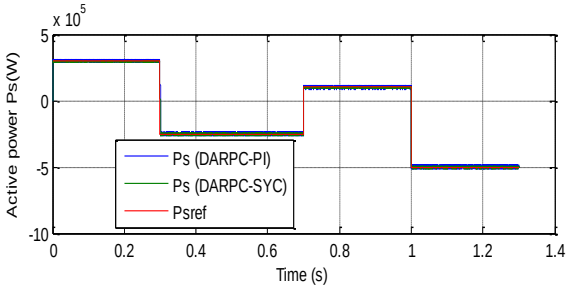

Figure 11. Active power

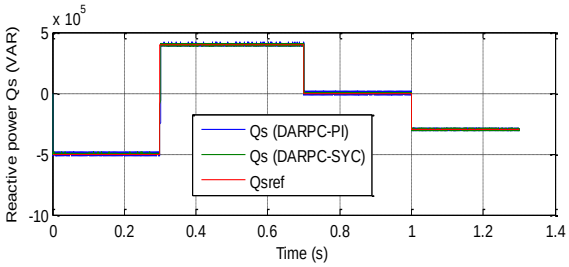

Figure 12. Reactive power

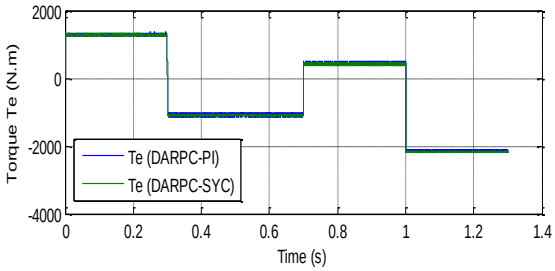

Figure 13. Torque

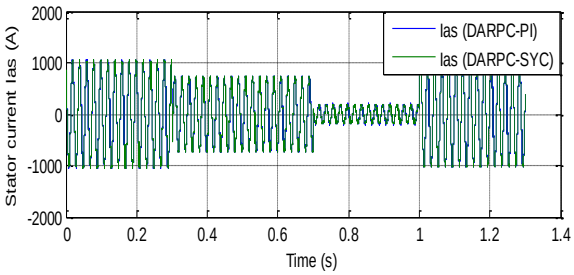

Figure 14. Stator current

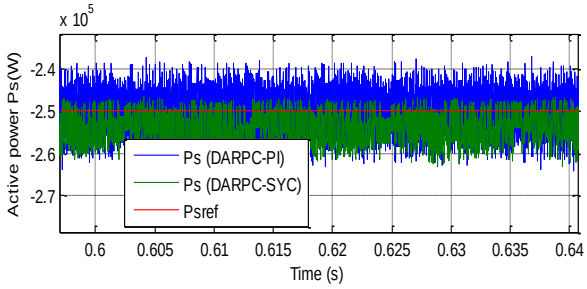

Figure 15. Zoom in the active power

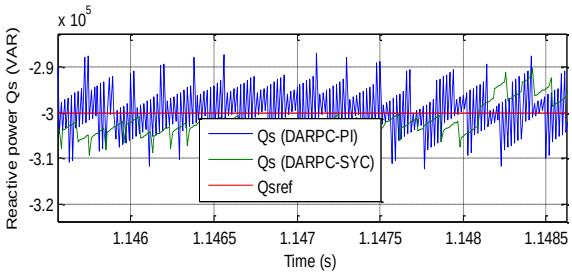

Figure 16. Zoom in the reactive power

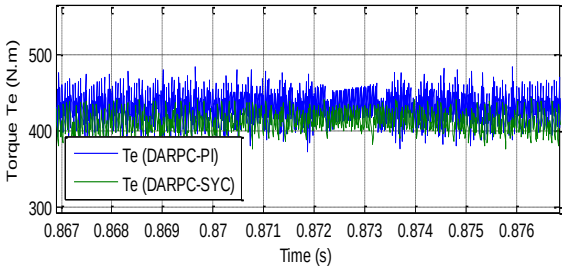

Figure 17. Zoom in the torque

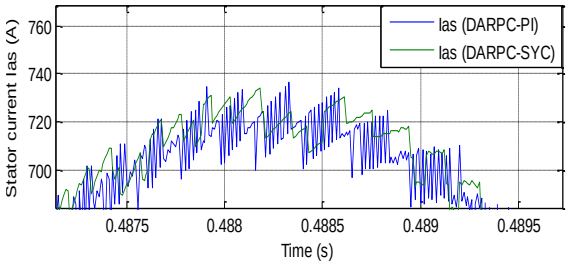

Figure 18. Zoom in the current

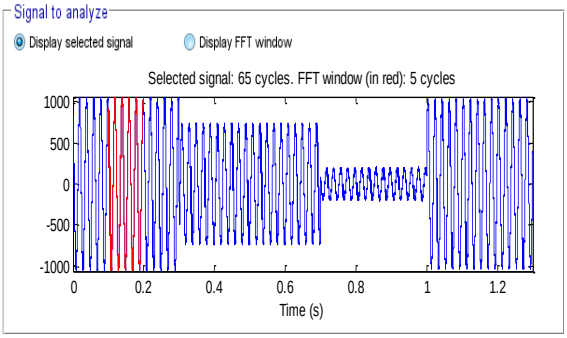

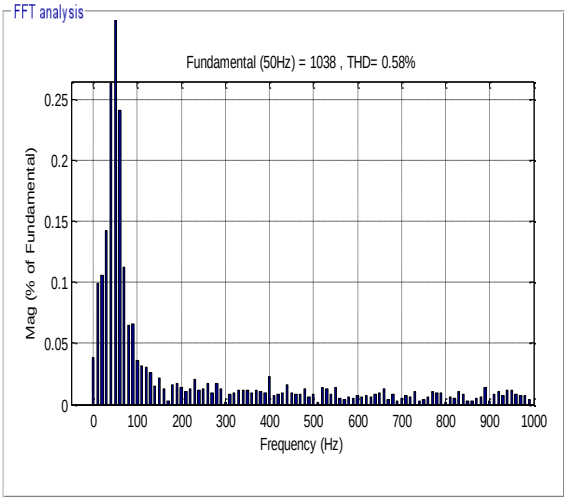

Figure 19. THD value of stator current (DARPC-PI)

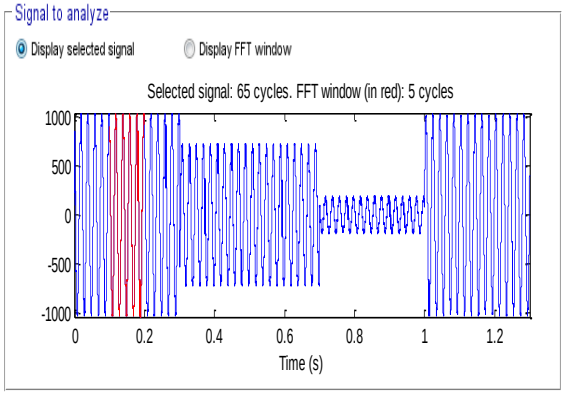

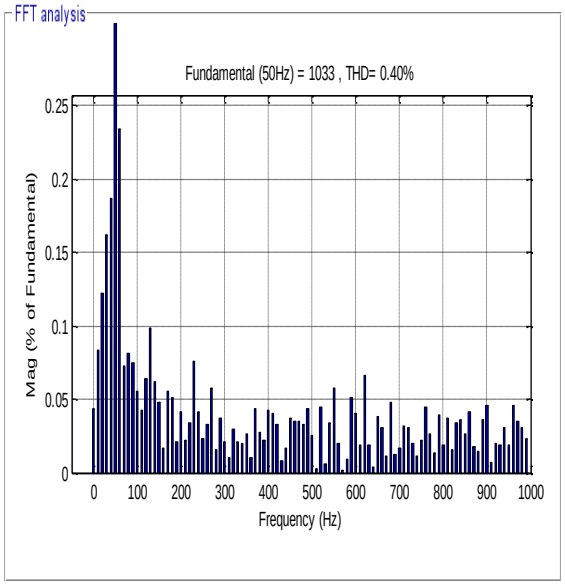

Figure 20. THD value of stator current (DARPC-SYC)

B. Second Test

In this second test, the nominal values of L_r and L_s are multiplied by 0.5, R_r and R_s are multiplied by 2. The results obtained are shown in Figures 21-30. As it's shown by these figures, these variations present an apparent effect on active power, torque, stator current, and reactive power such as the effect appears more significant for the DARPC with PI controllers compared to the DARPC-SYC technique (Figures 25-28). On the other hand, the DARPC-SYC technique minimized more the THD value of current compared to the DARPC with PI controllers (Figures 29-30). It can be concluded that the DARPC-SYC technique is more robust than the DARPC with PI controllers.

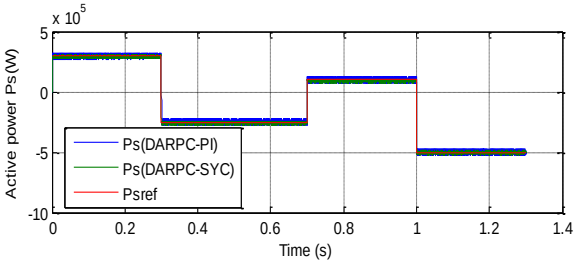

Figure 21. Active power

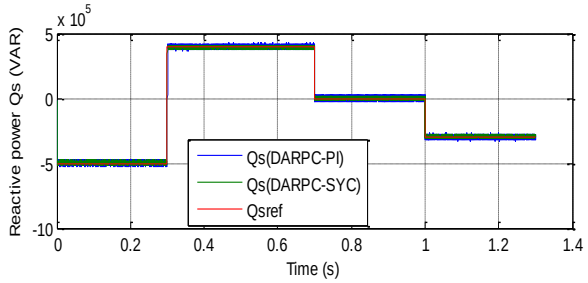

Figure 22. Reactive power

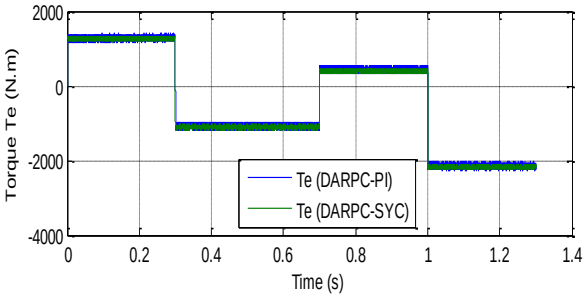

Figure 23. Torque

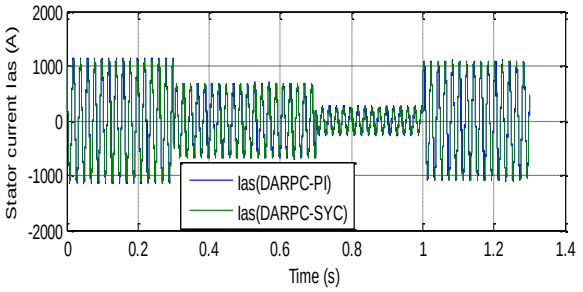

Figure 24. Stator currant

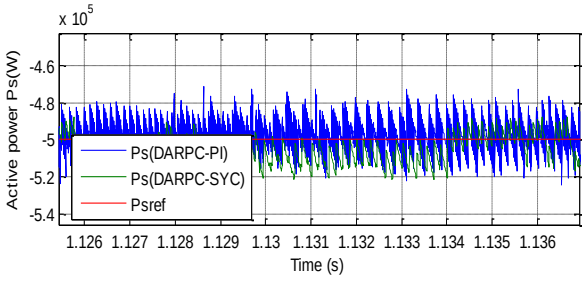

Figure 25. Zoom in the active power

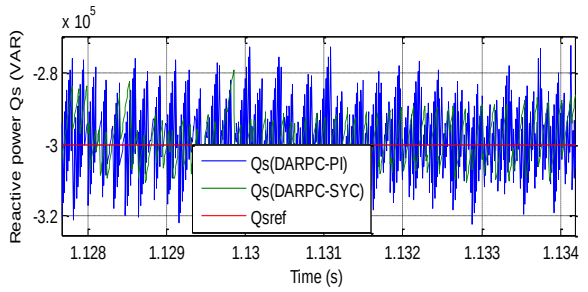

Figure 26. Zoom in the reactive power

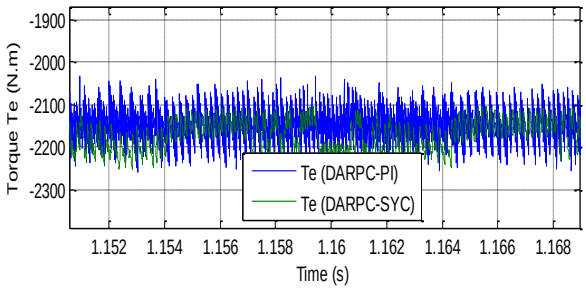

Figure 27. Zoom in the torque

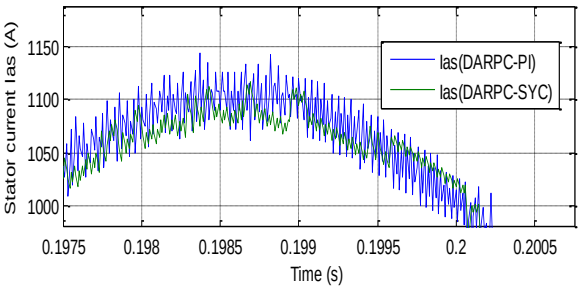

Figure 28. Zoom in the current

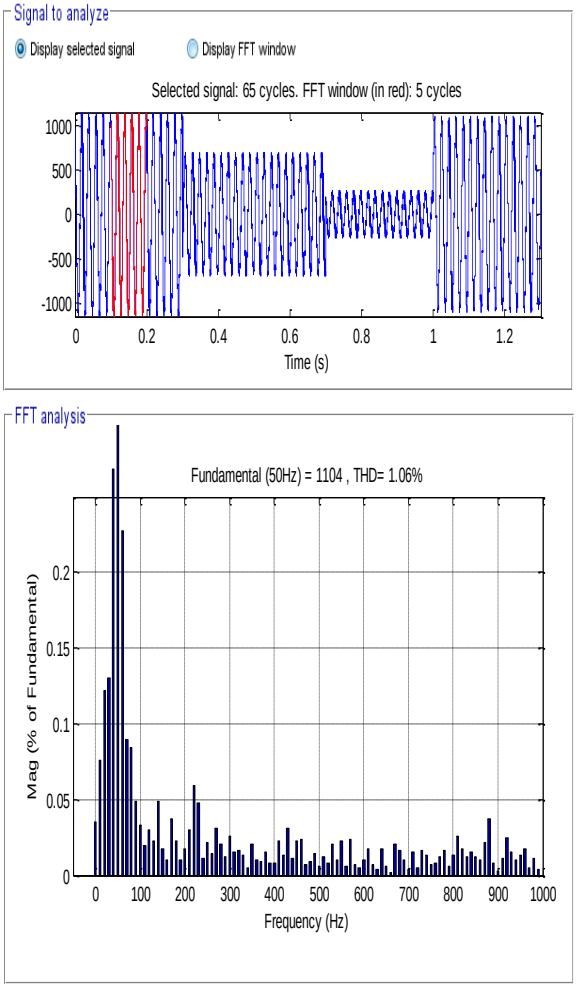

Figure 29. THD value of stator current (DARPC-PI)

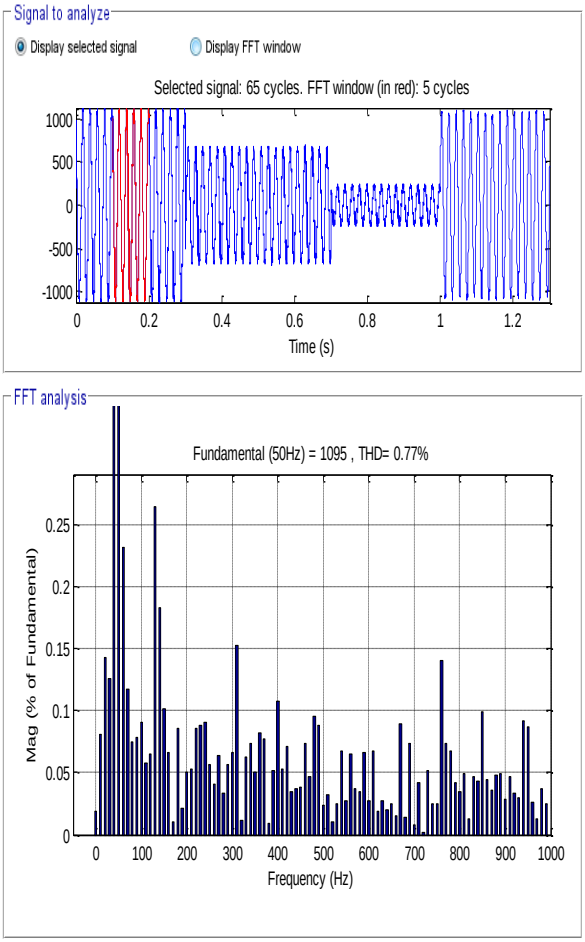

Figure 30. THD value of stator current (DARPC-SYC)

CONCLUSION

In this work, a robust technique is proposed to improve the effectiveness of the DARPC technique of the ASG driven by a variable speed DARPC system. Synergetic control is proposed to replace the traditional PI controllers. Synergetic controllers are designed to generate the direct and quadrature rotor voltages based on the reactive and active powers errors. The proposed technique preserves the advantages of the traditional DARPC technique such as fewer parameters dependence and simplicity. The performance of the proposed technique and DARPC with PI controllers is studied under power reference variation and machine parameters. By comparing the effectiveness of the designed technique with DARPC using PI controllers. It can conclude that the designed technique has a fast transient response under reference power variation conditions. The designed technique has superior performance with parameter variation. In addition, the proposed technique gives torque, current, active and reactive power waveforms with small ripples.

APPENDIX

The ASG used in our work has the following parameters: 380/696V, P_{sn}=1.5 MW, p=2, 50Hz, R_r = 0.021 Ω, R_s = 0.012 Ω, L_r = 0.0136H, L_m = 0.0135H, L_s = 0.0137H, J = 1000 kg.m^2 and f_r = 0.0024 Nm/s.

REFERENCES

[1] J. Qian, K. Li, H. Wu, J. Yang, X. Li, «Synergetic control of grid-connected photovoltaic systems, » International Journal of Photoenergy, Vol. 2017, pp. 1-11, 2017.

[2] Kondratiev, R. Dougal, G. Veselov and A. Kolesnikov, « Hierarchical control for electromechanical systems based on synergetic control theory, » 2009 IEEE Control Applications, (CCA) & Intelligent Control, (ISIC), St. Petersburg, 2009, pp. 495-500, doi: 10.1109/CCA.2009.5280959.

[3] L. Xiao, L. Zhang, F. Gao and J. Qian, « Robust Fault-Tolerant Synergetic Control for Dual Three-Phase PMSM Drives Considering Speed Sensor Fault, » in IEEE Access, Vol. 8, pp. 78912-78922, 2020, doi: 10.1109/ACCESS.2020.2989821.

[4] S. Berkane and A. Tayebi, « Construction of Synergistic Potential Functions on SO(3) With Application to Velocity-Free Hybrid Attitude Stabilization, » in IEEE Transactions on Automatic Control, Vol. 62, No. 1, pp. 495-501, Jan. 2017, doi: 10.1109/TAC.2016.2560537.

[5] C. G. Mayhew and A. R. Teel, « Synergistic Hybrid Feedback for Global Rigid-Body Attitude Tracking on $\hbox{ SO }(3)^{\ast}$ ${\ssr {SO}}(3)^{\ast}$, » in IEEE Transactions on Automatic Control, Vol. 58, No. 11, pp. 2730-2742, Nov. 2013, doi: 10.1109/TAC.2013.2266852.

[6] C. Chen, Y. Chang and T. Tsao, « Dynamic Trajectory Tracking by Synergistic Dual-Stage Actuation and Control, » in IEEE/ASME Transactions on Mechatronics, Vol. 22, No. 6, pp. 2600-2610, Dec. 2017, doi: 10.1109/TMECH.2017.2749510.

[7] R. S. Butt, I. Ahmad, R. Iftikhar and M. Arsalan, « Integral Backstepping and Synergetic Control for Tracking of Infected Cells During Early Antiretroviral Therapy, » in IEEE Access, Vol. 7, pp. 69447-69455, 2019, doi: 10.1109/ACCESS.2019.2907201.

[8] R. Prasad and N. P. Padhy, « Synergistic Frequency Regulation Control Mechanism for DFIG Wind Turbines With Optimal Pitch Dynamics, » in IEEE Transactions on Power Systems, Vol. 35, No. 4, pp. 3181-3191, July 2020, doi: 10.1109/TPWRS.2020.2967468.

[9] R. Ettouil, K. Chabir, M. N. Abdelkrim, «Optimal synergetic control for wind turbine system, » The International Journal of Engineering and Science, Vol. 7, No. 5, pp. 44-48, 2018.

[10] A. Kanchanahruthai, E. Mujjalinvimut, « Application of Adaptive synergetic control to power systems with super conducting magnetic energy storage system, » International Journal of Innovative Computing, Information and Control, Vol. 13, No. 6, pp. 1873-1885, 2017.

[11] A. Yahi, L. Barazane, «Improving speed performances of induction motor by using synergetic control theory, » IJST, Transactions of Electrical Engineering, Vol. 39, No. E2, pp. 183-192, 2015.

[12] M. Zhao, T. Wang, «A sliding mode and synergetic control approaches applied to permanent magnet synchronous motor, » Journal of Physics: Conf. Series 1087 042012, pp. 1-13, 2018.

[13] Y. Gui, M. Li, J. Lu, S. Golestan, J. M. Guerrero and J. C. Vasquez, « A Voltage Modulated DPC Approach for Three-Phase PWM Rectifier, » in IEEE Transactions on Industrial Electronics, Vol. 65, No. 10, pp. 7612-7619, Oct. 2018, doi: 10.1109/TIE.2018.2801841.

[14] M. Malinowski, M. Jasinski and M. P. Kazmierkowski, « Simple direct power control of three-phase PWM rectifier using space-vector modulation (DPC-SVM), » in IEEE Transactions on Industrial Electronics, Vol. 51, No. 2, pp. 447-454, April 2004, doi: 10.1109/TIE.2004.825278.

[15] P. Xiong and D. Sun, « Backstepping-Based DPC Strategy of a Wind Turbine-Driven DFIG Under Normal and Harmonic Grid Voltage, » in IEEE Transactions on Power Electronics, Vol. 31, No. 6, pp.

4216-4225, June 2016. Doi: 10.1109/TPEL.2015.2477442.

[16] Y. Gui, Q. Xu, F. Blaabjerg and H. Gong, « Sliding mode control with grid voltage modulated DPC for voltage source inverters under distorted grid voltage, » in CPSS Transactions on Power Electronics and Applications, Vol. 4, No. 3, pp. 244-254, Sept. 2019, doi: 10.24295/CPSSTPEA.2019.00023.

[17] H. A. Hamed, A. F. Abdou, M. S. E. Moursi and E. E. EL-Kholy, « A Modified DPC Switching Technique Based on Optimal Transition Route for of 3L-NPC Converters, » in IEEE Transactions on Power Electronics, Vol. 33, No. 3, pp. 1902-1906, March 2018, doi: 10.1109/TPEL.2017.2743230.

[18] S. Gaur, J. Acharya and L. Gao, « Enhancing ZF-DPC Performance with Receiver Processing, » in IEEE Transactions on Wireless Communications, Vol. 10, No. 12, pp. 4052-4056, December 2011, doi: 10.1109/TWC.2011.101211.111244.

[19] Y. Gui, M. Li, J. Lu, S. Golestan, J. M. Guerrero and J. C. Vasquez, « A Voltage Modulated DPC Approach for Three-Phase PWM Rectifier, » in IEEE Transactions on Industrial Electronics, Vol. 65, No. 10, pp. 7612-7619, Oct. 2018. Doi: 10.1109/TIE.2018.2801841.

[20] Andreas Giannakis, Athanasios Karlis, Yannis L. Karnavas, « A combined control strategy of a DFIG based on a sensorless power control through modified phase-locked loop and fuzzy logic controllers, » Renewable Energy, vol.121, pp.489-501, 2018.

[21] Jafar Mohammadi, Sadegh Vaez-Zadeh, Saeed Afsharnia, and Ehsan Daryabeigi, « A Combined Vector and Direct Power Control for DFIG-Based Wind Turbines, » IEEE Transactions on Sustainable Energy, Vol. 5, No. 3, pp.767-775, July 2014.

[22] H. Benbouhenni, "Twelve sectors DPC control based on neural hysteresis comparators of the DFIG integrated to wind power, " Tecnica Italiana-Italian Journal of Engineering Science, Vol. 64, No. 2, pp. 223-236, 2020.

[23] Djilali Kairus, René Wamkeue, Bachir Belmadani, Mustapha Benghanem, « Variable Structure Control of DFIG for Wind Power Generation and Harmonic Current Mitigation, » Advances in Electrical and Computer Engineering, Vol. 10, No. 4, pp.167-174, 2010

[24] A. Ramkumar, K. Karthi, K. Rajesh, « Review of Coordinated Control Strategy for Hybrid Type Wind Farms Under Network Faults, » International Journal of Advanced Science and Technology, Vol.29, No.04, pp. 4143-4152, 2020. Retrieved from http://sersc.org/journals/index.php/IJAST/article/view/24792.

[25] B. Habib, et al., «DPC based on ANFIS super-twisting sliding mode algorithm of a doubly-fed induction generator for wind energy system, » Journal Européen des Systèmes Automatisés, Vol. 53, No. 1, pp. 69-80, 2020.

[26] A. Yahdou, B. Hemici, Z. Boudjema, « Second order sliding mode control of a dual-rotor wind turbine system by employing a matrix converter, » Journal of Electrical Engineering, Vol. 16, No. 3, pp.1-11, 2016.

[27] A. Yahdou, B. Hemici, Z. Boudjema, «Sliding mode control of dual rotor wind turbine system, » The Mediterranean Journal of Measurement and Control, Vol. 11, No. 2, pp. 412-419, 2015.

[28] A. Yahdou, A. B. Djilali, Z. Boudjema, F. Mehedi, «Improved vector control of a counter-rotating wind turbine system using adaptive backstepping sliding mode, » Journal Européen des Systèmes Automatisés, Vol. 53, No. 5, pp. 645-651, October, 2020.

[29] H. Benbouhenni, Z. Boudjema, A. Belaidi, "Power Control of DFIG in WECS Using DPC and NDPC-NPWM Methods," Mathematical Modelling of Engineering Problems, Vol. 7, No. 2, pp. 223-236, 2020.

[30] B. Habib, " A comparative study between NSMC and NSOSMC strategy for a DFIG integrated into wind energy system, " Carpathian Journal of Electronic and Computer Engineering, Vol. 12, No. 1, pp. 1-8, 2019.

[31] H. Benbouhenni, Z. Boudjema, A. Belaidi, "Indirect vector control of a DFIG supplied by a two-level FSVM inverter for wind turbine system, " Majlesi Journal of Electrical Engineering, Vol. 13, No. 1, pp. 45-54, 2019.

[32] H. Benbouhenni, "Intelligence indirect vector control of a DFIG based wind turbines," Majlesi Journal of Electrical Engineering, Vol. 13, No. 3, pp.27-35, 2019.

[33] H. Benbouhenni, Z. Boudjema, A. Belaidi, "Using four-level NSVM technique to improve DVC control of a DFIG based wind turbine systems, " Periodica Polytechnica Electrical Engineering and Computer Science, Vol. 63, No. 3, pp. 144-150, 2019.

[34] B. Habib, "Application of five-level NPC inverter in DPC-ANN of doubly fed induction generator for wind power generation systems," International Journal of Smart Grid, Vol. 3, No. 3, pp. 128-137, 2019.

[35] H. Benbouhenni, Z. Boudjema, A. Belaidi, « Sensorless twelve sectors implementation of neural DPC controlled DFIG for reactive and active powers ripples reduction, » Majlesi Journal of Energy Management, Vol. 7, No. 2, 2018.

[36] H. Benbouhenni, Z. Boudjema, A. Belaidi, « Power ripple reduction of DPC DFIG drive using ANN controller, » Acta Electrotechnica et Informatica, Vol. 20, No. 1, pp.15-22, 2020.

[37] B. Habib, « A direct power control of the doubly fed induction generator based on the three-level NSVPWM technique, » International Journal of Smart Grid, Vol. 3, No. 4, 2019.

[38] T. Ademoye, "Decentralized synergetic control of power systems," These de Doctorate, College of Engineering and Mineral Resources at West Virginia University, 2012.